

Tests of the adaptive optical system with a modified correlation sensor at the big solar vacuum telescope

V.P. Lukin,^{1,2} V.M. Grigor'ev,³ L.V. Antoshkin,¹
 N.N. Botygina,¹ O.N. Emaleev,¹ P.A. Konyaev,¹ E.A. Kopylov,²
 V.V. Lavrinov,¹ P.G. Kovadlo,³ and V.I. Skomorovskii³

¹*Institute of Atmospheric Optics,
 Siberian Branch of the Russian Academy of Sciences, Tomsk*

²*Tomsk State University*

³*Institute of Solar-Terrestrial Physics,
 Siberian Branch of the Russian Academy of Sciences, Irkutsk*

Received January 30, 2007

Tests of the modified correlation sensor (MCS) at Big solar vacuum telescope (BSVT) have shown that at a proper choice of the filtering function parameters, the MCS reliably measures shifts of the solar granulation image in the telescope first focus under good visibility conditions. The MCS, as a part of the adaptive optical system, was intended for measuring the image shift in the telescope second focus. It turned out that the image quality becomes noticeably worse at image transfer to the second focus. The MCS measures the image shift of solar granulation in the second focus only under extremely good visibility conditions and certain granulation structure. Reduction of the telescope entrance aperture to 170 mm insignificantly affects the image quality and, therefore, the MCS operation.

Introduction

Studying small scale physical processes on the Sun requires solar telescopes with high spatial or angular resolution. As known¹ solar atmosphere is highly structured and dynamic. Two important scales determine the structure of solar atmosphere: the high-altitude pressure scale and the photon free path. In the solar photosphere, both of them are about 70 km or about 0.1" in angular measure. In order to resolve these fundamental scales, the telescope angular resolution should be better than 0.1". Investigations of such phenomena as heating of solar corona, solar activity, and variations of solar emittance affecting the Earth climate, require the observations for the magnetic field microstructure in the solar atmosphere with the angular resolution better than 0.1". Constructing theoretical models of the solar atmosphere requires the parameters, which can be obtained in studying the behavior of the objects having even smaller spatial scales.

To improve spatial resolution of the operating solar telescopes those are equipped with adaptive optical (AO) systems. The AO systems for solar telescopes are more complicated than those for the stellar systems. The main difficulties are caused by the fact that daytime turbulence is stronger, quality of vision essentially varies in time, and the wave front sensor should operate with the visible radiation from low-contrast, extended, time-varying objects such as solar granulation. Because of heating the Earth's surface heating by direct light the near-ground turbulence is much stronger at daytime. Even in better locations at typical telescope height from 20 to 40 m above the ground, the typical value of the Fried radius r_0 equals

to 10 cm ($\lambda = 500$ nm). Moreover, the Fried radius characterizing the strength of atmospheric turbulence, undergoes strong fluctuations of short time scales (seconds) and often reduces to several centimeters. Therefore, in spite of the relatively small dimensions of entrance apertures of solar telescopes, the solar AO systems require greater number of high-speed correction elements as compared to the stellar ones.

The main problem in the development of solar AO systems is the wave front sensor. A sensor used for stellar AO systems, cannot be used for the solar ones, since the Sun is an extended object, and the objects, which can be used as reference stars (natural or laser) for the nighttime AO systems,² are inapplicable, when the Sun is observed. The solar AO systems use, as objects for tracking, the structures on the sun disk like sunspots, pores, and solar granulation. Granulation, in particular, is the target too problematic for tracking, since the granulation pattern has low contrast and varies in time scales about 1 min.

It should be noted that application of a laser reference star (LRS) is not an efficient solution for the solar adaptive optics (AO), since the lasers needed for operation against the solar disk background are to be very bright or extremely narrow-band pass filters must be used. Complexity and cost of such projects are inaccessible. Possible application of LRS in solar astronomy could be the observation of a very weak corona. The corona brightness makes approximately 10^{-6} of the disk brightness. The future use of LRS in the solar AO system is considered for the corona observation with a new ATST (Advanced Technology Solar Telescope) 4-meter-diameter telescope.

The dynamics of solar AO at first stages of its formation is described in detail in the study by Rimmele.¹ The first experiments on solar AO were carried out by Hardy at Vacuum Tower Telescope (VTT) in 1979 at Sacramento Peak. The shear interferometer was used in the experiment as a wave front sensor. It was assumed that the AO system could operate both with bright stars and with sunspots. Actually, the AO system has demonstrated the improvement of star image quality, however, failed to improve the sunspot image.

The first operating solar AO system was put into operation by the Lockheed company in the middle of 80s on the basis of a 19-element segmented mirror and the analog wave front sensor of Shack–Hartman (SH) with 19 quadrant detectors for recording the image shears formed by 19 subapertures. The system could use quite contrast, against the general background, single pores and sunspots as the objects for tracking. In the real experiment at Dunn Solar Telescope (DST) in Sacramento Peak, it was shown that the image quality can be improved by including AO system into the solar telescope and this was an important milestone in the development of solar AO systems.

The next stage in solar AO system development was the design of the correlation wave front sensors capable of using a fragment of solar granulation as an object for tracking.³ Inclusion of AO systems with a correlation sensor as components of the operating solar telescopes arranged in the best locations allows the contrast of solar granulation image to be increased, however, the diffraction-limited resolution can only be achieved under conditions of perfect visibility ($r_0 = 20$ cm). Thus, at New Swedish Solar Telescope (NSST) with aperture of 97 cm installed in La Palma the granulation images are obtained near the sunspot with resolution of 0.1" (70 km) due to the AO system and postdetection processing. The filter with a central wavelength at 430 nm was used in the experiment. The frame exposure time was equal to 20 ms.

Improvement of the granulation pattern quality at solar telescopes operating under worse visibility conditions still remains a difficult task. In 2001, we have carried out tests of the AO system with a correlation sensor at BSVT of the Baikal Astrophysical Observatory.⁴ The system used the images of quite contrast sunspots as objects for tracking. In 2003, after the improvement of the image recording system (replacement of the video camera with an 8-bit analog-to-digital converter by the video camera with a 12-bit analog-to-digital converter), the AO system showed good results, when using the image fields with a small pore as an object for tracking, whose contrast was about 10%. The technological CCD-array characteristics of the video camera used didn't enable us to obtain similar results with the granulation pattern fragment. It happened so that not only the hardware of the wave front sensor, but also of the correlation algorithm used should be modified.

We have developed a modified correlation algorithm⁵ based on analysis of films recorded during the expedition in 2004, which was tested in measuring

solar granulation image shear. The validity of shear measurements by the modified correlation sensor (MCS) was checked by comparison with that measured using traditional sensor of image fragments successfully operating with traditional correlation algorithm.

In this paper we present results of MCS test in the experiments at BSVT.

Modified correlation sensor and test procedure

The solar granulation image, as an object for observations is inherently low-contrast physical structure. Instrumental errors of solar telescopes and atmospheric turbulence essentially reduce the granulation pattern contrast.^{6,7} In addition the image transfer to the second focus by means of additional optical elements in real schemes of solar telescopes with the AO system also reduces the granulation pattern contrast. All this causes special requirements to the systems of image recording and shear meters. The well-known method of smoothing illumination over the image field at operation of the AO system with low-contrast images requires high-precision preliminary measurements. We have tested^{3,8} a filtration method, which, in our opinion, is more efficient in the region of spatial frequencies of the images recorded. In case of a proper choice of the filter function (FF) parameters, this method allows one to remove the image illumination inhomogeneity formed by the image forming optics (low spatial frequencies), and the image defects, whose dimension is comparable with the dimensions of the receiver's array elements (high frequencies). In our case, these are the technological features of the CCD-array (four horizontal lines of elements with sensitivity in 0.4 to 1.2% below the sensitivity of the rest array elements) and random defects that may appear in the process of measurements.

The modified FFT algorithm⁷ is implemented for calculation the mutual correlation function (MCF) in the image shear sensor:

$$C(i, j) = \sum_{l=0}^{N-1} \sum_{m=0}^{M-1} I(l, m) I_R(i+l, j+m),$$

$$C = F^{-1} \{ F^+ [I] F^+ [I_R] \},$$

$$C_m = F^{-1} \{ F^+ [I] F^+ [I_R] H(\kappa_x, \kappa_y) \};$$

$$H(\kappa_x, \kappa_y) = \exp \left\{ -a \left[(\kappa_x - \kappa_{x0})^2 + (\kappa_y - \kappa_{y0})^2 \right] \right\},$$

where F denotes the Fourier transform; I is the distribution of illumination over the image; $H(\kappa_x, \kappa_y)$ is the filter of spatial frequencies κ_x and κ_y with the parameter a characterizing its width.

The filter parameters H are selected based on the experimental conditions to provide the necessary sharpness of the MCF peak.

The testing of MCS with the modified correlation algorithm of the image jitter measurement was carried out at BSVT in September of 2005. Optical arrangement of the setup is presented in Fig. 1.

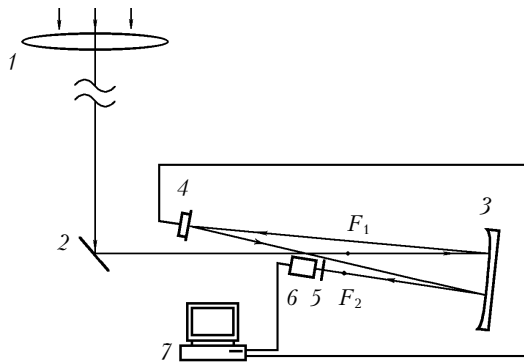


Fig. 1. Optical arrangement of the experimental setup: 1 is the telescope objective of the BSVT ($D = 760$ mm, $F = 40$ m); 2 is the diagonal mirror; 3 is the spherical mirror ($F = 4$ m); 4 is the controllable mirror; 5 are the filters; 6 is a «DALSTAR» video camera (128×128 pixels, 12-bit ADC, 490 frames/s); 7 is a computer (Pentium VI, 2.4 GHz with a PC-DIG video card).

The software consisted of an auxiliary tuning program and the main control program. The control program, in its turn, had several operation modes, i.e., measurement, tracking, and recording. When the main program run in the measurement mode, the stream of frames from the video camera was represented in the overlay window of the capture driver. The correlation sensor of image shear generated the results in real time in both digital and graphic form. In the tracking mode, the control signals came through the controller with RS-232 interface to the piezoelectric drive⁹ for the x - y control of angular position of the mirror 4. The recording mode was intended for storing video signals in computer memory for its subsequent processing. The sequence of 128×128 pixels frames, in the format of 16 bit/pixel, was first recorded to the RAM and then to a hard disc.

In a real scheme of the AO system, the MCS operates with the image formed near the second focus F_2 (see Fig. 1). However, the test program of MCS included the image shear measurements both in the second and in the first focus of the telescope in order to check the serviceability of the modified algorithm at objects with different contrast and noise level.

Tests were carried out according to the following procedure. A fragment of a solar granulation image was selected by means of the optical system tuning. We have determined the typical structure dimensions of the image and selected the FF-parameters, which were then introduced into the control program. We have checked out the MCS operation with the selected image fragment. Viewing and analysis of MCF as well as the moving image fragment were carried out in real time, in the adjacent windows, on the monitor screen. If the selected FF-parameters specify a well-defined correlation function maximum tracking for the image shear, the measurements of image fragment were carried out. Files of the measured shears and images of reference and averaged frames were formed. A movie with the same image fragment was recorded for the subsequent analysis. If the MCS operated with the image fragment formed in the second focus,

the shear measurements were conducted in two modes: with closed control loop and without control.

Results on MCS test in the first focus of the telescope

The modified correlation algorithm has shown good results at operation with fragments of the solar granulation images with the well-defined structure with 1.2 to 2.0% contrast (Fig. 2). The fragments of solar granulation images were obtained in the first focus under good weather conditions on September 24, 2005 (light northern wind without gusts 2–5 m/s, cloudless sky, meteorological visual range 8–10 km) and on September 25, 2005 in the first half of the day (south wind 0.5–1 m/s, thin layer of cirrus clouds, meteorological visual range 8–10 km). Angular image dimension is 26×26" (128×128 pixels). Angular field of view of the sensor was 20×20" (96×96 pixels).

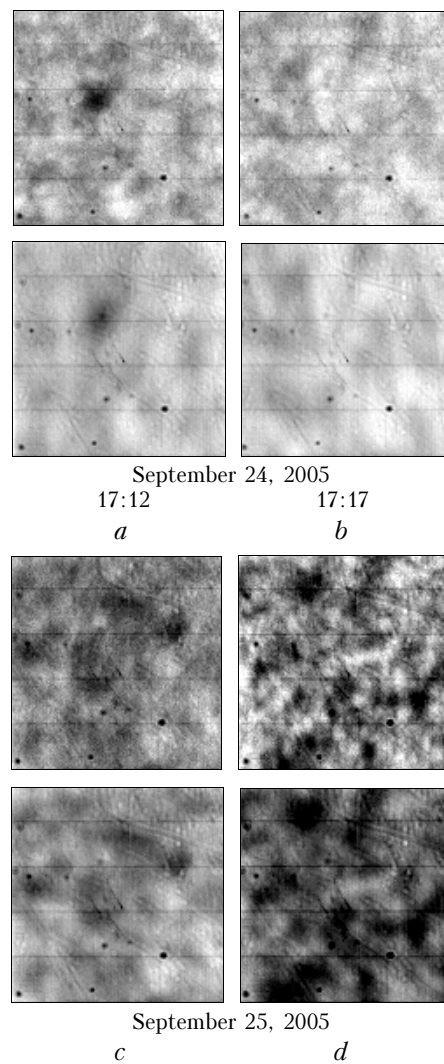


Fig. 2. Fragments of solar granulation images. The upper series denote images obtained with the frame exposure time equal to 2.04 ms; lower series denote the frames averaged over 1000 frames taken in a period of 6.12 ms.

Figure 3 shows the cross section of one of the presented images. Such images of solar granulation are obtained in the experiment at first focus of the telescope under good visibility conditions.

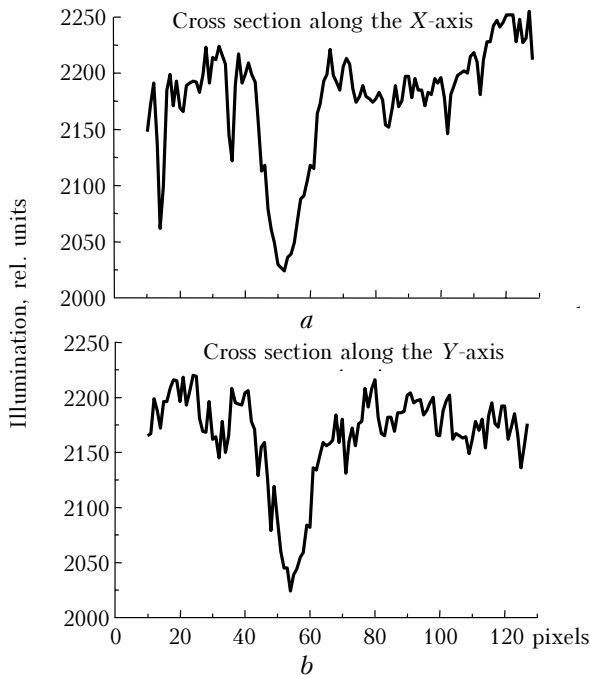


Fig. 3. Orthogonal sections across the pore image (see Fig. 2a, upper series), 1 pixel = 0.21".

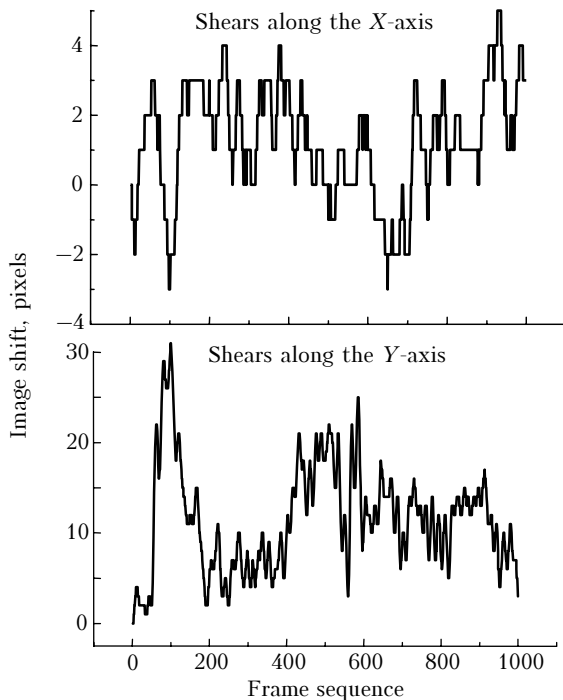


Fig. 4. Image fragment shears of solar granulation measured in real time. Duration of a single realization was 6.1 s (1000 frames with exposure time of 2.04 ms with a period of 6.12 ms).

Use of the modified correlation algorithm in image shear measurements of solar granulation recorded in a movie allows estimating the validity of

the FF-parameters selection in shear measurements of the same fragment in real experiment. The image shear of the same solar granulation fragment measured in real time (September 24, 2005, 17:17) and in a movie (September 24, 2005, 17:23), are presented in Figs. 4 and 5.

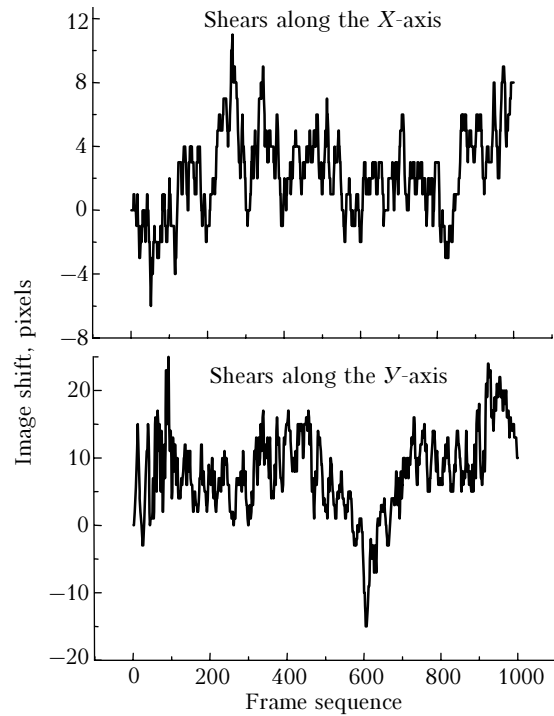


Fig. 5. Image shears of solar granulation measured in a movie. Duration of the realization was 16.32 s (1000 frames with the exposure time of 2.04 ms with a period of 16.32 ms).

The measurements were conducted by MCS with identical FF-parameters: normalization parameter a was equal 0.5, typical structure dimension l_0 equals 16 pixels. The window of the MCS analysis is 96×96 pixels that corresponds to the angular image dimension 20×20".

Having the selected FF-parameters, the correlation function had a well-defined maximum moving with the image. Visual estimation of the image shear from the presented frames (Fig. 6) and comparison with the measured values has shown that the MCS well tracks the image shear.

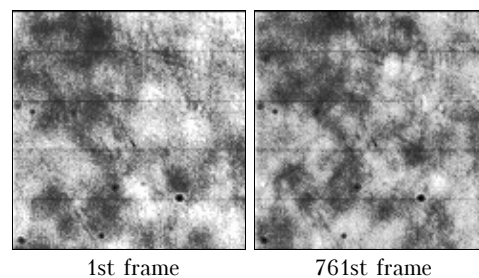


Fig. 6. Frames from the movie. The image contrast in the window of 761st frame analysis was 1.47%. Interval of contrast variation in the movie varied from 1.3 to 1.6%.

A possibility of changing the FF-parameters of MCS at image measurement in the same movie allows analyzing the spread of measured shear values with the parameter selection criterion used (Fig. 7).

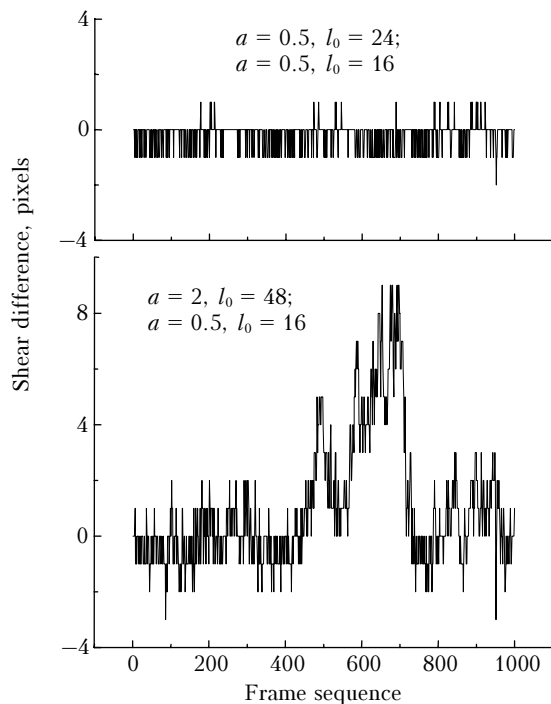


Fig. 7. Difference of measured image shears in the movie (September 24, 2005, 17:23) at different FF-parameters.

If the FF maximum is moved by one harmonics, the spread of measured values covers the interval of $[-1, 1]$ pixels. If larger elements of the image structure are isolated from the same fragment as objects for tracking, the measured shears would essentially differ. Probably, valid shear measurement can be performed if the largest possible sharpness and magnitude of the moving maximum of MCF are found for the fragment selected. As l_0 parameter, it is necessary to choose the size of the most contrast elements of the image structure. Its size should be several times smaller than that of analysis window and an order of magnitude larger than the size of immobile structure elements caused by the defects of the receiver. The FF half-width is determined by the spread of sizes of most contrast structure elements and their variation in the process of recording.

Recording and processing of long realizations of the image shear allow estimation to be done of the Fried radius characterizing the atmospheric turbulence from the image jitter variance. To estimate the Fried radius, the realizations were selected with no instrumental image jitter due to wind vibrations of a siderostat mirror occurred. The measurements were carried out under conditions of low wind (about 0.5 m/s speed) along the axis of the siderostat mirror support.

Figure 8 presents the reference frame and frame averaged over the realization (September 25, 2005,

09:59), whose duration was 50.12 s (8192 frames with the frame exposure time of 2.04 ms). In the image shear measurements, the MCS was used with the following FF parameters: $a = 0.5$, $l_0 = 16$ pixels. The root-mean-square deviation of the image shear along the X -axis was equal to 3.47 pixels (0.730") and 3.52 pixels (0.740") along the Y -axis. Atmospheric turbulence causing such image shears is characterized by the Fried radius equal to 3.7 cm ($\lambda = 500$ nm).

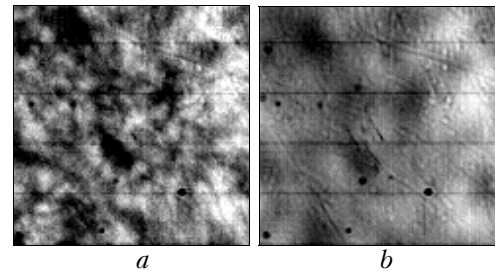


Fig. 8. Reference frame (a) and frame averaged over the realization (b).

Note that the Fried radius estimation by the formula proposed in the Ref. 6 connecting the granulation pattern contrast in telescopes with diameter less than 1 m and the Fried radius, if it is smaller than 10 cm, agrees with the value obtained from the image jitter variance. It should be noted that quality of solar granulation image in these measurements was one of the best observed in expeditions in August–September during the period from 1998 to 2005.

Results on MCS test in the second focus of the telescope

Tests of MCS in the second focus as a component of the AO system were carried out on September 22, 2005 and on September 23, 2005. Structure of the solar granulation image (Fig. 9) observed using full entrance aperture of the telescope and the same angular size of the detector's field of view differed from the image the MCS dealt with in the first focus.

Review and analysis of movies recorded in the second focus, have shown that image structure varies during the two-second long realization. Thus low-contrast large inhomogeneities of the illumination appear at some moments, while at other moments in time there appear small image structures (Figs. 9b and d). In real experiment, in the process of image fragment stabilization, its structure also varies and at some moments either large or small structure elements manifest themselves most strong. The AO system is unstable. In the realization presented in Fig. 10 the adaptive system tries tracking the large scales.

The small scales of illumination distribution of the recorded frames lead to the tracking breakdown (emissions from single points are presented in Fig. 10b). The Table demonstrates the root-mean-square deviations of the above-mentioned realizations, which help estimating the stabilization efficiency of the image fragment in the second focus.

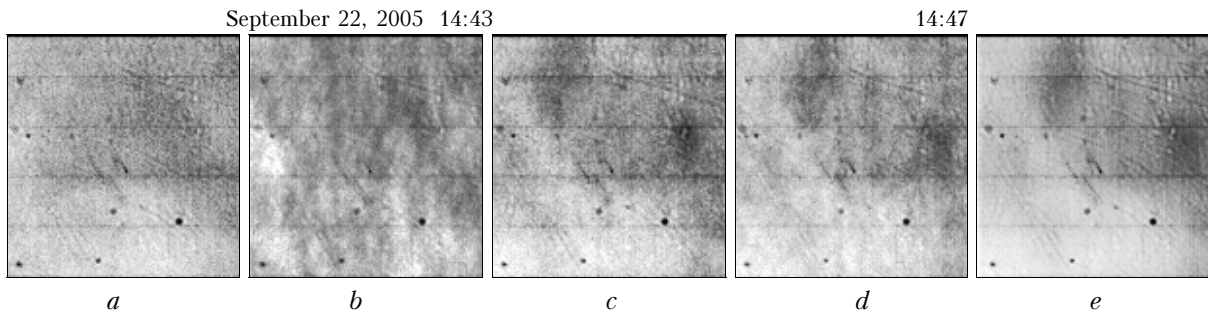


Fig. 9. Images obtained in the second focus: *a* and *b* are the reference frames from real measurements; *c* and *d* are the 1st and 232nd frames from the movie; *e* is the image averaged over 1000 frames of the movie taken with the frame rate of 490 frame/s.

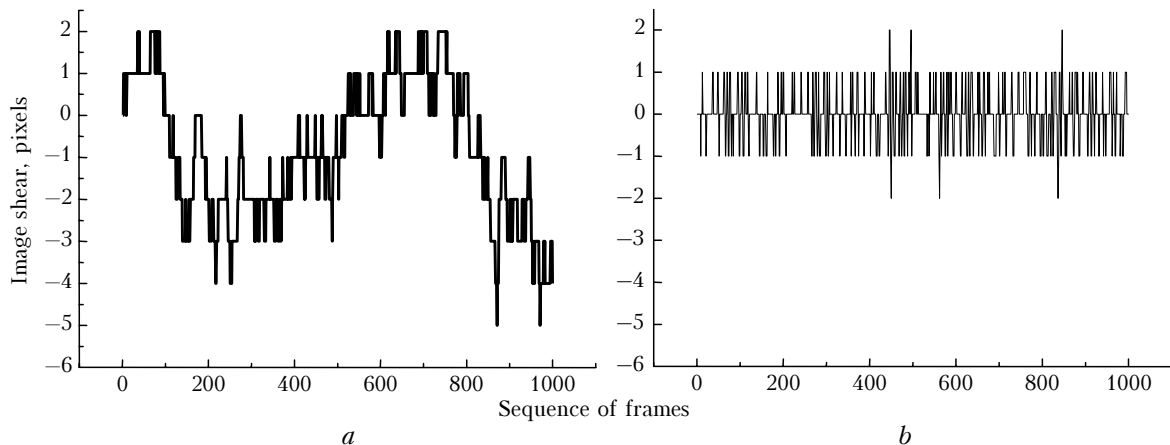


Fig. 10. Image shear along the *X*-axis in measurements performed on September 22, 2005 (14:43) at open (*a*) and closed (*b*) control loops in separating the large scales: ($a = 1$, $l_0 = 32$ pixels). 1 pixel = 0.21", the duration of a single realization was 6.10 s (1000 frames with exposure time of 2.04 ms with a period of 6.12 ms).

Statistical estimate, pixel	Image shear at open control loop	Image shear at stabilization	Control signal	Image shear in the movie
Mean value	-0.822	0.002	2.094	-2.89
Root-mean-square deviation	1.64	0.61	2.84	1.98
Minimum value	-5	-2	-4	-8
Peak value	2	2	10	0

Tests of MCS at different diameters of the telescope entrance aperture

The development of investigations on AO at BSVT assumes formation of the system correcting not only the total wave front tilts, but also aberrations of the higher orders. The telescope entrance aperture is broken into subapertures by the objective Hartmann mask. The image shears made by each aperture are recorded. The tests of MCS were carried out at reduction of the entrance aperture diameter. The telescope entrance aperture was reduced by the diaphragm mounted in front of the telescope lens either at its center or at its side edge. We analyzed the quality of solar granulation image in the second focus and image shears measured with the MCS. At reduction of the entrance aperture diameter to 170 mm, the quality of solar granulation image in the

second focus changes insignificantly. In the recorded realizations (1000 frames with exposure time of 2.04 ms), only large-scale varying image structure is observed, the well-defined small-scale structure manifests itself only in some frames (Fig. 11).

From the movie recorded with the diaphragm of 220-mm diameter, it is clear that MCS produces spikes at frames with image structure different from the structure of the reference frame. This situation is illustrated in Figs. 12 and 13. In MCS, we used the FF with the same parameters as in the case with full aperture.

At image stabilization, such error of MCS can lead to the increase in control signal essentially exceeding the upper boundary of the controllable mirror. The mirror takes the extreme position and, therefore, the tracking error increases by the shear caused by this extreme position of the mirror. The control signal goes on to grow (integral control law) and the system does not catch the stabilization mode.

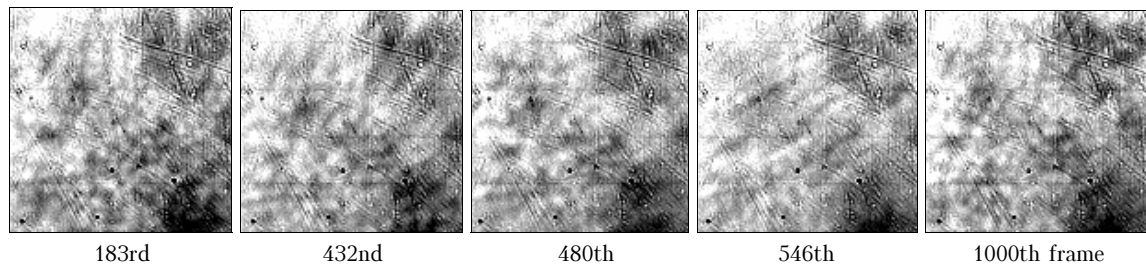


Fig. 11. Frames with small-scale image structure in the movie taken on September 23, 2005 (13:50) (diaphragm diameter of 170 mm in the center of the telescope lens).

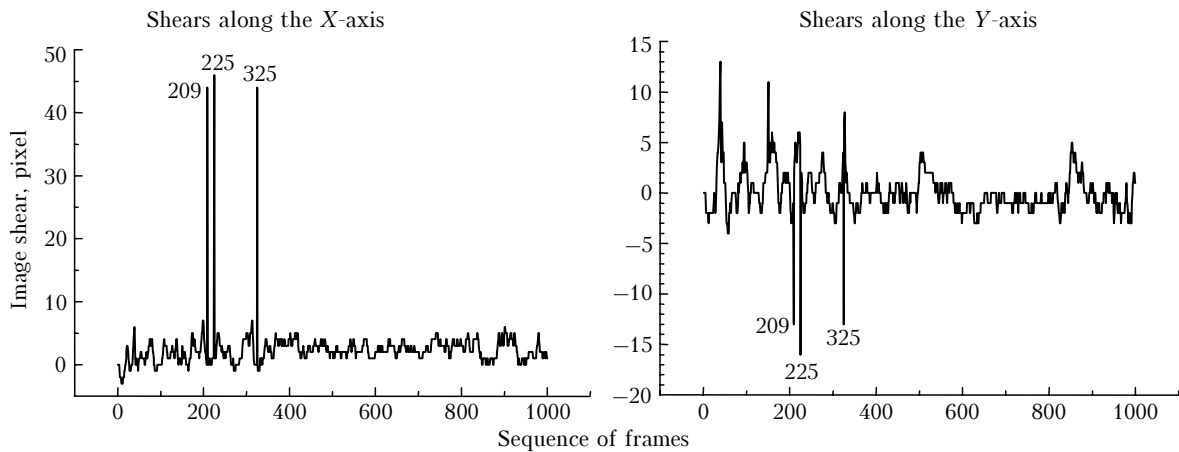


Fig. 12. Image shear from the movie taken on September 23, 2005 (13:12) with the diaphragm diameter of 220 mm at the telescope lens's edge (FF-parameters are: $a = 1$, $l_0 = 32$ pixels).

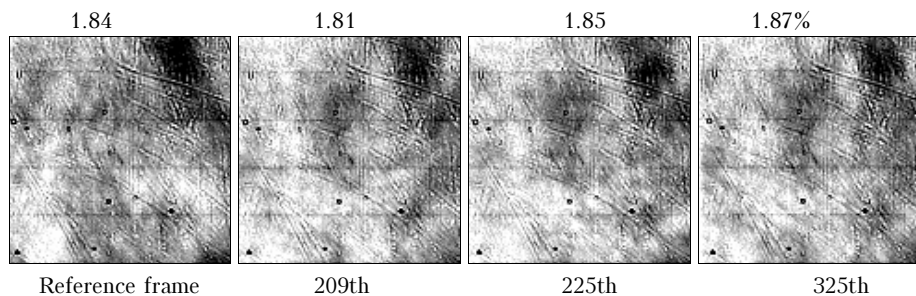


Fig. 13. Frames of the movie taken on September 23, 2005 (13:12) and image contrast.

Such a situation occurred in real measurements (13:05) (Figs. 14 and 15*a* and *b*). In the next realization (13:06), the image structure varied insignificantly, the measurement error was lower and the image stabilization was much better. (Fig. 15*c* and *d*).

Conclusions

Use of MCS for measuring the image shear at the first focus of the telescope has shown that at a proper selection of the FF parameters, the MCS reliably measures the image shear of solar granulation under very good visibility conditions.

As a part of AO system, the MCS measures the image shear at the second focus only at high quality of solar granulation image (only under good visibility conditions and at certain granulation structure). Reducing diameter of the telescope entrance aperture

to 170 mm insignificantly affects the image quality and, therefore, the MCS operation.

Appreciable image deterioration takes place at image transfer to the second focus. At present, the AO system elements are arranged outside the vacuum telescope tube on the holographic table in the room where temperature drops can happen. The optical path length at image transfer from the telescope first focus to the second one, makes approximately 17 m. Distortions produced by the additional optical elements and the medium between them essentially affect the quality of the initially low-contrast image of solar granulation. The image structure in the second focus changes during the short realizations (2 s). The MCS algorithm tries tracking the large scales (diffuse image) and causes the large error at separation of small scales by the FF (small-scale image structure seldom manifested itself in the course of measurements).

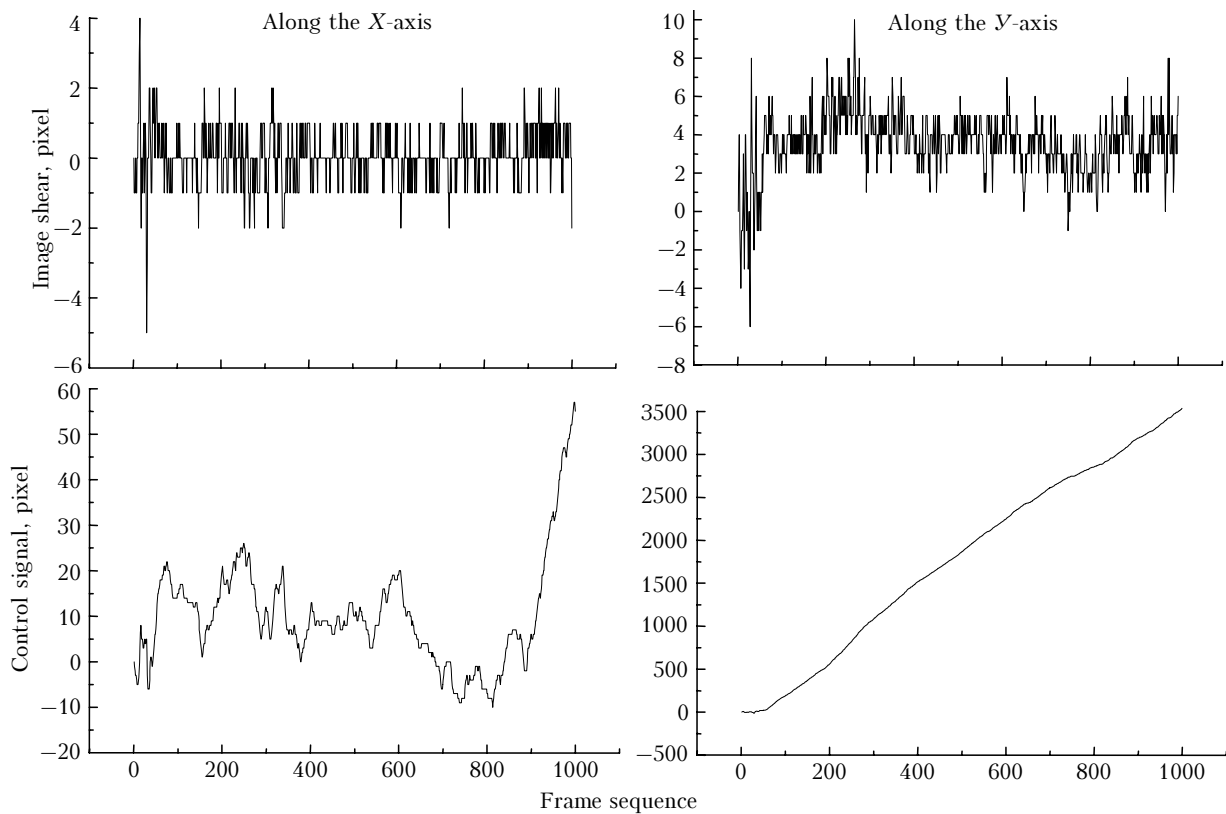


Fig. 14. Image shears and control signals in real measurements with closed control loop (13:05).

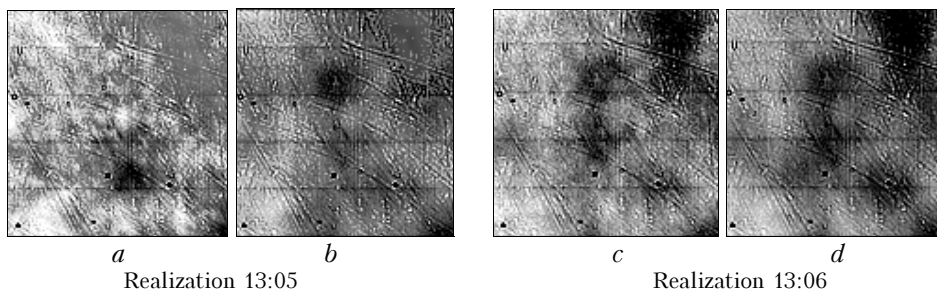


Fig. 15. Reference (*a*, *c*) and average (*b*, *d*) frames during the stabilization.

In developing the AO system at BCVT, correcting the solar granulation image, it is necessary to take measures to provide the high quality of the optical system, which transfers the image to the second focus.

Acknowledgements

This work was supported in part within the limits of the complex integration project of SB RAS No. 3.2 "Development of adaptive systems of image correction for the ground telescopes" and of the Presidium Program RAS No. 16. Part 3. Project 1. "Daytime astroclimate and the problems of adaptive telescope construction".

References

1. T.R. Rimmele, Proc. SPIE **4007**, 218–231 (2000).
2. V.P. Lukin, Usp. Fiz. Nauk **176**, No. 9, 1000–1006 (2006).
3. O.von der Luhe, A.L. Widener, Th. Rimmele, G. Spence, R.B. Dunn, and P. Wiborg, Astron. and Astrophys. **224**, 351–360 (1989).
4. L.V. Antoshkin, N.N. Botygina, O.N. Emaleev, P.G. Kovadlo, P.A. Konyaev, V.P. Lukin, A.I. Petrov, and A.P. Yankov, Atmos. Oceanic Opt. **15**, No. 11, 934–937 (2002).
5. L.V. Antoshkin, N.N. Botygina, O.N. Emaleev, P.G. Kovadlo, P.A. Konyaev, V.P. Lukin, and V.V. Lavrinov, Atmos. Oceanic Opt. **18**, No. 12, 969–974 (2005).
6. G. Ricort and C. Aime, Astron. and Astrophys. **76**, 324–335 (1979).
7. G. Ricort, C. Aime, C. Roddier, and J. Borgino, Sol. Phys. **69**, 223–231 (1981).
8. V.P. Lukin, L.V. Antoshkin, N.N. Botygina, O.N. Emaleev, V.M. Grigor'ev, P.A. Konyaev, P.G. Kovadlo, V.I. Skomorovskii, and A.P. Yankov, Opt. Zh. **73**, No. 3, 55–60 (2006).
9. L.V. Antoshkin, N.N. Botygina, O.N. Emaleev, P.A. Konyaev, V.P. Lukin, and A.P. Yankov, Prib. Tekh. Eksp., No. 1, 144–146 (2002).